4-10-2009

The Effects of Diameter Fluctuations and Coiling on the Sensitivity of Sapphire Single Crystal Optical Fiber Evanescent Wave Fluorescence Sensors

Jimmy Ray Gamez
University of South Florida

The Effects of Diameter Fluctuations and Coiling on the Sensitivity of Sapphire Single Crystal Optical Fiber Evanescent Wave Fluorescence Sensors

by

Jimmy Ray Gamez

A thesis submitted in partial fulfillment
of the requirements for the degree of
Master of Science
Department of Physics
College of Arts and Sciences
University of South Florida

Major Professor: Nicholas Djeu, Ph.D.
Dennis Killinger, Ph.D.
Matthias Batzill, Ph.D.

Date of Approval:
April 10, 2009

Keywords: fiber optics, chemical sensor, evanescent field, tapered fiber, coiled fiber

DEDICATION

I dedicate this work to my parents, Gil and Diane Gamez, whose teachings and immeasurable support have made this accomplishment possible; my brother, Michael Milbrath, whose expectations have kept me motivated over the years; and my best friend, Casey Mugwhy Wisner, whose inspiration has driven me to success.

ACKNOWLEDGMENTS

I would like to thank Dr. Nicholas Djeu for giving me the opportunity to discover what I'm capable of; my committee members, Dr. Dennis Killinger and Dr. Matthias Batzill, for their time and advice; Mary Ann Prowant for always taking care of me as my mom away from home; Kimberly Carter and Daisy Matos for their extraordinary support and assistance; Bobby Hyde for his expert SEM training and assistance; Feibing Xiong and Hui Chen for their lively discussions and culture sharing; and last but not least, Dr. Jermaine Kennedy for his support, advice, and laughs.

TABLE OF CONTENTS

LIST OF TABLES

LIST OF FIGURES

The Effects of Diameter Fluctuations and Coiling on the Sensitivity of Sapphire Single Crystal Optical Fiber Evanescent Wave Fluorescence Sensors

Jimmy Ray Gamez

ABSTRACT

The purpose of this research was to determine the effect of diameter fluctuations on the sensitivity of sapphire multimode optical fibers used as evanescent wave fluorescence sensors. It was predicted that fluctuations in the diameter of the fiber would act as a series of bi-tapers converting lower order modes to higher order modes increasing the evanescent wave penetration depth thereby increasing the excitation of a cladding of fluorescent fluid. Induced fluorescence from the fluid cladding would then couple back into the fiber more efficiently increasing the sensitivity of the sensor.

The effect of coiling the fiber on the sensitivity of the sensor was also explored. Coiling the fiber converts lower order modes into higher order modes and increases the sensing length while maintaining a small probe size. However, coiling experiments produced unexpected results and in the course of studying these results a layer of material was discovered coating the surface of the sapphire fibers.

CHAPTER 1

INTRODUCTION

1.1 History of Optical Fibers

In today's era of modern marvels and seemingly boundless access to information, it is not difficult, or uncommon, to take for granted the natural phenomena that allow our society to grow and prosper. We owe our lives, health, and ways of life to Nature herself. One of the great achievements of our society was to harness the natural phenomenon of light; that mysterious entity that knows no time, no mass, and yet travels at the upper bound of velocity. Not only does light heat our planet, grant us life, and provide us vision, light has also become the backbone of our communication system, improved our healthcare system, and advanced our industry. The ability to confine and channel light through optical fibers has been one of the major breakthroughs in the harnessing of light energy.

Using light to carry information dates back to prehistoric times when fires were used to send signals over a distance[1]. In 1854, John Tyndall demonstrated that sunlight could be guided in a stream of water poured from a bucket. He understood that this total reflection was a consequence of exceeding the limits of refraction[2]. The phenomenon of total internal reflection was used by William Wheeler in 1880 who designed a series of pipes that guided sun light into a building lighting its rooms[1]. Wheeler's "light pipes" were a precursor to modern fiber optics. In the interest of medicine and communications,

research was continued by pioneers such as Baird and Hansell, Lamm, van Heel, Hopkins and Kapany, and Hirschowitz in an effort to increase the efficiency of light guided by means of internal reflection. By 1960 glass-clad optical fibers were used in medical endoscopy but were not efficient for long distance communications. However, with the advent of the laser in the 60s, the realization of fiber optics' potential by Kao and Hockham sparked a flurry of research across the globe to establish efficient fiber optic communications[3].

While the majority of optical fiber research and development has been focused on improving optical fibers' design for communication purposes, one branch of research has instead focused on using optical fibers as local environment sensors. Fiber optic sensors are typically divided into two groups: intrinsic sensors and extrinsic sensors[4]. Intrinsic sensors provide information about the local environment via interactions that take place within the fiber. Examples of intrinsic sensors are fiber optic gyroscopes based on the Sagnac effect and seismic/vibration sensors based on changes in the optical path length of the guided light in response to deformations in the fiber due to vibrations. In contrast, for extrinsic sensors, the interactions take place outside of the fiber. Extrinsic sensors can be used to monitor temperature, pressure, displacement, and chemical reactions.

It is obvious that the ability to confine and guide light through optical fibers was a great achievement for society. Fiber optics are not only crucial to our communications system but also vital to health care and industry. Fiber optic sensors can be implemented in all areas of industry where conventional sensors are inefficient, outdated, or non-existent.

1.2 Conventional Optical Fibers

For communications applications, extensive research and development time has been devoted to manufacturing optical fibers with the highest quality and precision to ensure the lowest possible attenuation over distance. Optical fibers are typically made using fused silica, plastics, or unique materials depending on the desired characteristics. A common optical fiber design is shown in Figure 1.1.

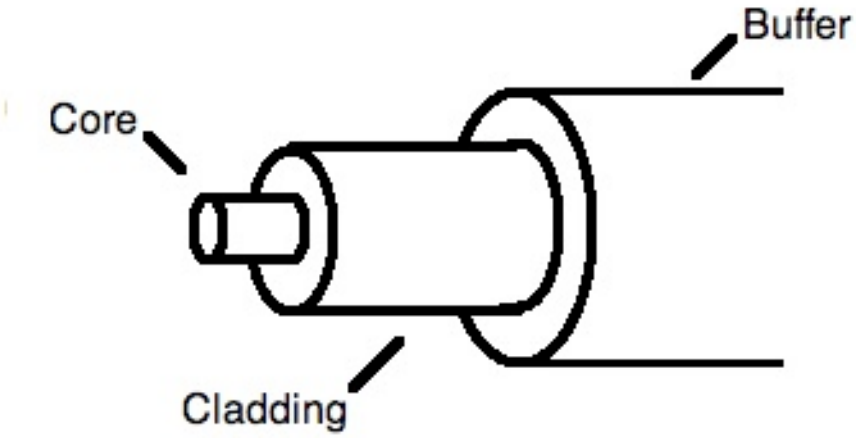

Figure 1.1 – Optical Fiber Design

The core and cladding begin as preform rods that may be an inch in diameter that are stretched and pulled into fibers as thin as a few tens of microns and kilometers in length. The fibers are coated with a protective buffer to add mechanical strength.

To make possible total internal reflection, the index of refraction of the cladding is chosen to be lower than that of the core. A ray representation of light guided in an optical fiber is shown in Figure 1.2.

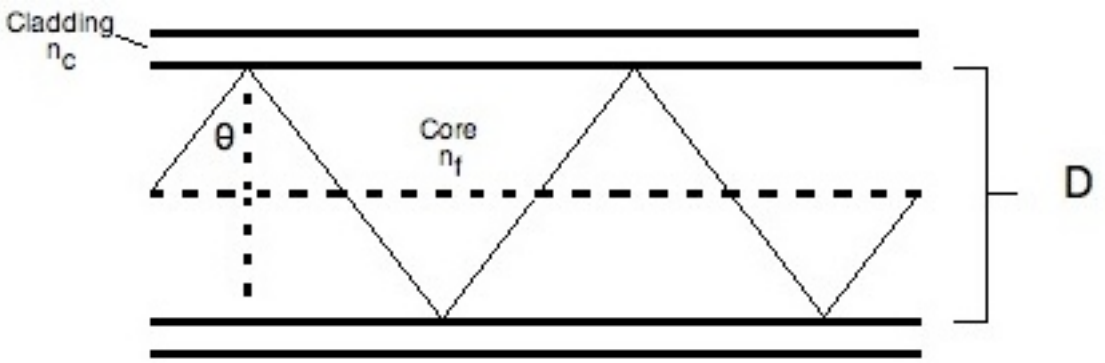

Figure 1.2 – A Single Ray Propagating in an Optical Fiber

This figure depicts a meridional ray; a ray which traverses the fiber in a plane containing the fiber's optic axis. Rays can also traverse the length of the fiber following a "helical" path around the central axis. These rays are termed skew rays[5]. For the sake of simplicity, only meridional rays will be considered. It is obvious that rays can be incident on the core/cladding interface at an infinite number of angles with respect to the interface normal. However, rays with angles smaller than the critical angle of total internal reflection are refracted out of the core and lost[6]. Rays with angles larger than the critical angle totally reflect from the interface and bounce along the length of the fiber. The critical angle is given by

$$\theta_c = \sin^{-1}\left(\frac{n_c}{n_f}\right) \tag{1.1}$$

where n_f is the index of refraction of the core and n_c is the index of refraction of the cladding. The number of reflections per unit length is given by

$$N = \frac{\cot(\theta)}{D} \tag{1.2}$$

1.3 Sapphire Optical Fibers

Sapphire (Al_2O_3) is a single crystal material with an index of refraction of approximately 1.76 and is known for its chemical resistance and high melting point (approximately $2000^{O}C$) making it an ideal material for chemical sensing in extreme environments. Sapphire optical fibers are unique because their process of manufacturing prohibits an effective method of applying a cladding layer; the entire fiber is the core. This characteristic immediately lends itself convenience to be used as an evanescent chemical sensor.

Single crystal sapphire optical fibers used for this research were grown using the laser heated pedestal growth (LHPG) method. A schematic of the growth apparatus is shown in Figure 1.3. Feed-stock of single crystal sapphire is raised into the focal point of a parabolically focused CO_2 laser beam creating a molten zone at the tip of the feed. A seed fiber is lowered and attached to the molten zone. The seed is then raised from the molten zone drawing a single crystal fiber. The diameter reduction ratio of the drawn fiber is determined by the rate at which the seed is pulled up depleting the molten zone and the rate at which the feed is raised replenishing the molten zone.

Since the seed and feed are both controlled by electric motors, it is possible that their action may not be completely smooth. Furthermore, while the laser is actively stabilized, power fluctuations still occur, leading to temperature changes in the molten zone. Either of these scenarios results in diameter fluctuations in the grown fiber. Great strides have been taken to eliminate these instabilities so as to grow fibers that have minimal diameter fluctuations.

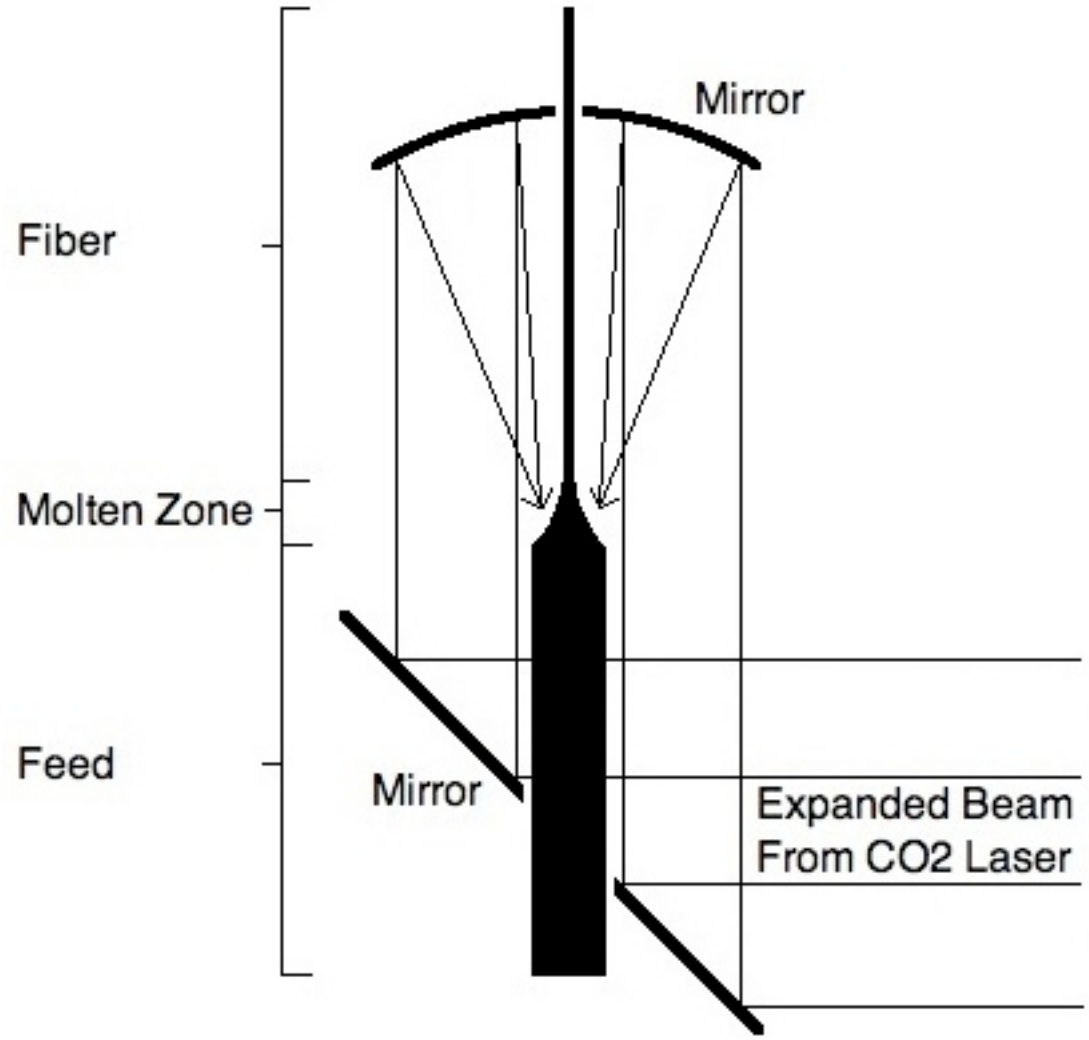

Figure 1.3 – Laser Heated Pedestal Growth (LHPG) Method

However, research has shown that tapering the sensing region of evanescent wave absorption sensors increases the sensitivity of the sensor[7, 8]. Previous works have involved removing the cladding from a conventional glass optical fiber, heating the exposed core, and stretching the fiber to create a bi-tapered sensing region. In the case of less than ideal sapphire fibers, the diameter fluctuation can be modeled as a series of bi-tapers.

The research presented in this thesis compares the sensitivity of sapphire fibers with varying degrees of diameter fluctuation when used as evanescent wave fluorescence chemical sensors. Also, the effects of coiling the sensing region on fluorescence sensitivity are explored. Previous works have demonstrated that bending or coiling the sensing region increases the sensitivity of evanescent wave absorption sensors[9, 10].

CHAPTER 2

THEORY

2.1 Evanescent Wave Fluorescence Sensing

Fluorescence sensing is a useful tool in the medical field and in industry. By detecting fluorescent markers, the presence of target chemicals and their concentrations can be determined. Fluorescent molecules absorb photons specific to their quantum energy level spacing and emit photons of a lower energy. Chemicals with known absorption and emission spectra can be identified using fluorescence sensing.

Evanescent wave fluorescence sensing utilizes the energy of an evanescent wave present at the core/cladding interface of an optical fiber. To satisfy boundary conditions at each reflection point at the interface, energy in the form of an evanescent wave penetrates into the cladding and decays exponentially to a depth of[11]

$$d_p = \frac{\lambda}{2\pi n_f \sqrt{\sin^2\theta - \sin^2\theta_c}} \tag{2.1}$$

where λ is the excitation wavelength and θ is the ray's angle of incidence with respect to the interface normal. According to this equation, the penetration depth increases as θ approaches θ_c.

Optical fiber chemical sensors have been developed that exploit the energy of this evanescent wave. However, to access the evanescent wave, the fiber must be stripped of its buffer and the cladding must be removed either mechanically or by chemical etching. The bare core can then be introduced to a gaseous or fluid environment that serves as an

effective cladding. Since sapphire fibers do not have a cladding, they can be conveniently exposed to a liquid environment that serves as an effective cladding. If this environment contains fluorescent molecules and the wavelength of the light traveling through the fiber matches the absorption spectra of these molecules, the evanescent wave at the core/liquid interface will excite the fluorescent molecules causing them to fluoresce at a wavelength specific to their emission spectra. It has been shown theoretically and experimentally that photons emitted on the low index side of the interface are able to couple back into the fiber and be guided within the core[12-16]. Carniglia and Mandel described this coupling pathway by modeling excited fluorescent molecules as oscillating electric dipoles that emit their own evanescent field[16]. This evanescent field extends into the core of the fiber and allows fluorescent photons to couple into the core and propagate within the fiber at angles larger than the fiber's critical angle.

According to equation 2.1, rays incident on the core/liquid interface with angles close to the critical angle penetrate deeper into the liquid allowing more fluorescent molecules to be excited thereby increasing the amount of coupled fluorescent light back into the fiber. Methods to increase the number of higher order modes include selective ray launching, tapering the sensing region, and bending or coiling the sensing region[7-10, 14, 15, 17, 18].

2.2 Theory of Ball Lens

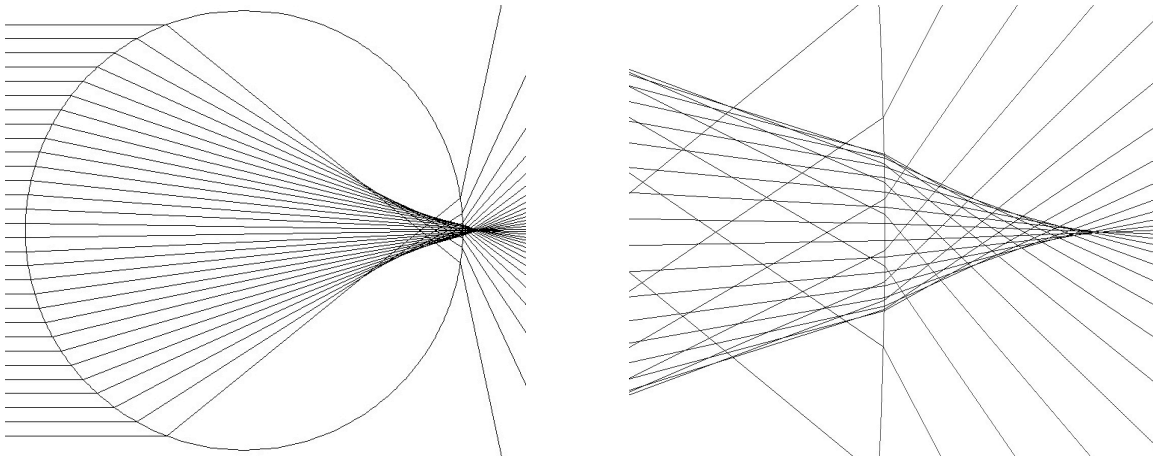

Figure 2.1 – Focal Behavior of 10mm Diameter LaSFN9 Ball Lens[19]

A 10mm diameter LaSFN9 ball lens was used to generate and launch high order modes into the fiber. Figure 2.1 shows a ray representation of the focusing behavior of the ball lens generated using the optical design software OSLO-EDU by Sinclair Optics[19]. The image on the left shows an expanded beam entering the ball lens while the image on the right is a close view of the focal region. It is obvious that due to spherical aberration, rays incident near the top and bottom of the lens will be tightly focused closest to the output face of the lens. These rays will enter the fiber with low angles, θ, maximizing the number of bounces per unit length and evanescent penetration depth. To generate these higher order modes, it was necessary to enlarge the beam diameter to efficiently fill the ball lens.

2.3 Diameter Fluctuations as a Series of Bi-tapers.

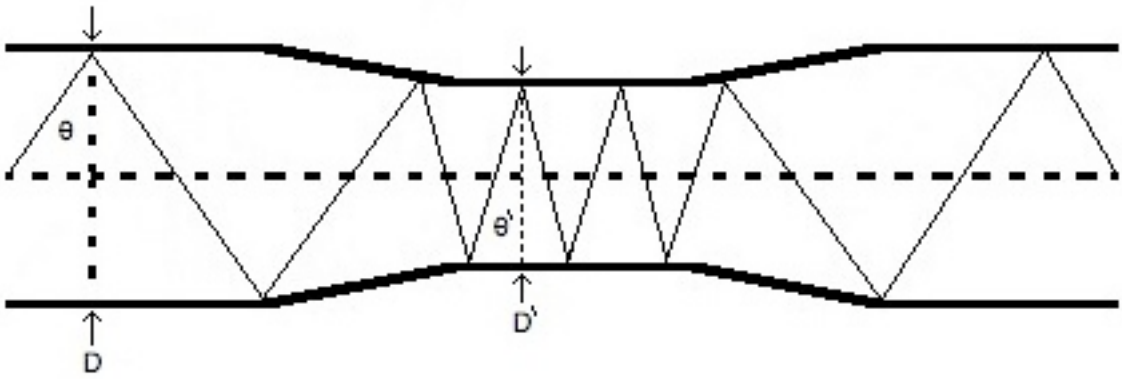

Figure 2.2 – Bi-tapered Evanescent Wave Sensor

It has been demonstrated that tapering or introducing a bi-taper into the sensing region of conventional fibers increases the sensitivity of the sensor in evanescent absorption sensing, evanescent surface plasmon resonance sensing, as well as evanescent fluorescence sensing[7, 8, 14, 15, 17]. In these studies, tapered sensors and bi-tapered sensors have been efficiently fabricated by removing the cladding from conventional fibers, heating the core, and stretching the fibers. As shown in Figure 2.2, the down-taper converts angle θ to a smaller angle θ' according to[11]

$$D\cos\theta = D'\cos\theta' \tag{2.2}$$

effectively increasing the penetration depth of the evanescent wave in the taper and narrow region of the probe.

Furthermore, in evanescent wave fluorescence sensing, the fluorescent photons at the interface must also efficiently couple back into the core of the fiber as guided modes. Studies have shown that the fluorescent molecules possess their own exponentially decaying evanescent wave that extends into the core thereby providing a coupling

pathway back into the core[12, 13, 16]. Also, the taper could allow non-evanescent fluorescent photons to couple back into the core and propagate with angles larger than the critical angle and thus be guided as shown in Figure 2.3.

It was the purpose of this thesis research to determine if the diameter fluctuations in less than ideal sapphire optical fibers would also increase the sensitivity when used as evanescent wave fluorescence sensors. The diameter fluctuations would essentially act as a series of bi-tapers increasing the penetration depth of the evanescent field and increasing the fluorescence coupling back into the fiber.

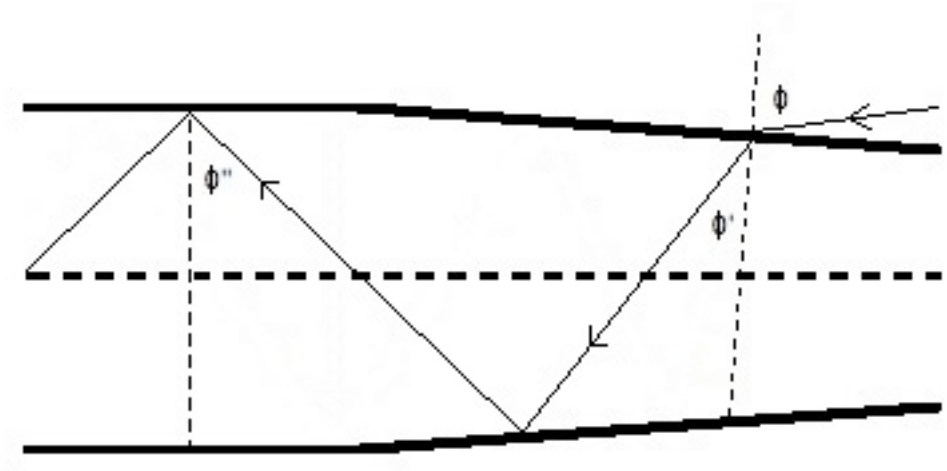

Figure 2.3 – Non-Evanescent Fluorescent Photon Coupling

2.4 Coiling

Studies have also shown that bending or coiling the sensor can increase the sensitivity of evanescent wave absorption sensors by converting lower order modes into higher order modes[9, 10]. Figure 2.4 depicts a ray representation of mode conversion within a bent fiber. Using ray geometrics, it can be seen that the bent region decreases the ray's angle with the interface normal thereby increasing the evanescent penetration depth as well as the number of bounces per unit length.

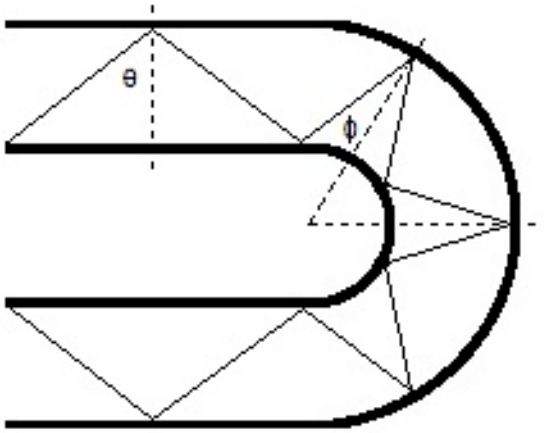

Figure 2.4 – Bent Fiber

Sapphire optical fibers can easily be coiled into many turns, which is convenient not only to increase the evanescent penetration depth and number of bounces but also to increase the length of the sensing region while minimizing the size of the probe.

CHAPTER 3

EXPERIMENTAL METHODS

3.1 Effect of Diameter Fluctuations on Sensitivity

The apparatus described in Figure 3.1 was used to experimentally determine the effect of diameter fluctuations on the sensitivity of the fiber sensor.

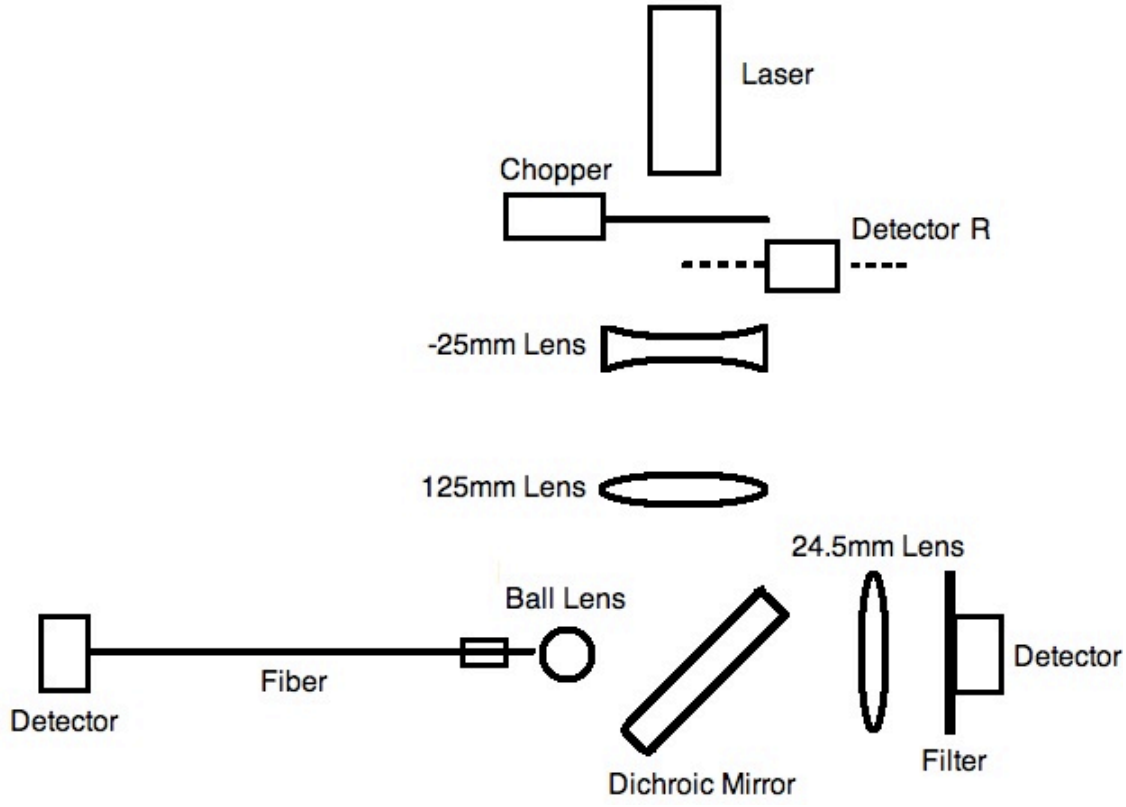

Figure 3.1 - Block Diagram of Apparatus

A frequency doubled Nd:YAG laser (532.4nm) was used as the excitation source chopped at 200Hz. The output power of the chopped beam was measured using a Newport Corporation silicon photodetector model 818-SL that could be dropped into the path of the beam immediately after the chopper. This detector was connected to a Newport Corporation 835 digital power meter and the signal from this meter was fed into a Tektronix TDS1002B oscilloscope that was set to average the signal over 128 samples. The oscilloscope was interfaced to a laptop computer that automatically collected the peak-to-peak voltage of the detector.

According to the theory of operation of the ball lens, the highest order modes would be generating by rays incident on the ball lens farthest from the center of the lens. Therefore, it was necessary to enlarge the beam diameter to fill the ball lens. The most convenient and efficient lens combination was determined to be a 4mm beam generated by placing a -25mm focal length lens (KBC043) at the focal point of a 125mm focal length lens (KBX067). The lenses were 25.4 mm diameter, anti-reflection coated, BK7 lenses by Newport Corporation. The beam diameter was determined by following the accepted standard of measuring Gaussian beam spots: a 100-micron pinhole was scanned across the beam to determine the half intensity points of the spot. The distance between these points gave the full width at half maximum (FWHM) of the beam. Collimation was determined to be acceptable after measuring the beam diameter at two locations about one meter apart. The enlarged and collimated beam was incident at a 45-degree angle to a dichroic mirror which reflected the beam 90 degrees to the 1cm diameter LaSFN9 ball lens.

MicroMaterials Incorporated supplied several multi-mode single crystal sapphire fibers that were grown using the laser heated pedestal growth (LHPG) method. The ends of the fibers were polished and the input end was mounted in a 1cm capillary tube. A small drop of DucoCement fixed the fiber to the capillary tube. The tube was then fixed to a three way precision stage to easily orient the fiber tip to maximize the coupling between the focused beam and the fiber. Since the ball lens does not produce a single focal point, the fiber tip was positioned to maximize the transmission of the fiber. A custom machined fluid tub was placed beneath the fiber and a length of fiber was allowed to droop into the tub that could then be filled with fluid. A Newport Corporation silicon photodetector model 818-SL was placed at the output end of the fiber to measure the transmission of the fiber. To avoid stray and ambient light from being detected, the face of the detector was covered with thick, black paper except for a small pin hole in the center to admit the end of the fiber. This detector was connected to the power meter/ oscilloscope combination and the laptop computer recorded its peak-to-peak voltage.

On the opposite side of the dichroic mirror, a Newport Corporation 25.4mm diameter, BK7, 25.4mm focal length lens (KBX046) collected and focused the fluorescing signal through a filter to the element of a Thorlabs, Inc. PDA55 amplified silicon photodetector. To avoid noise from ambient light, the filter was pressed flush to the face of the detector and black cardboard was placed around the dichroic mirror, 25.4 mm lens, and Thorlabs detector. This detector was mounted on a three way precision stage to ensure proper alignment and was directly connected to the Tektronix oscilloscope.

Since the focal length of the ball lens was extremely short, it was impossible to directly monitor the power incident on the face of the fiber. At the initial stages of this research, the beam's power was measured with the detector pressed up to the ball lens and compared to the beam's power directly after the chopper. The power loss due to reflections and losses in the lenses was calculated and recorded.

It was also determined that the two Newport Corporation 818-SL photodetectors had slightly different measurements. This discrepancy between detectors was due to the improper calibration of the Newport Corporation 835 power meter. Ideally this meter would be factory calibrated to a single detector. However, only one meter was available and the detectors had to be connected one at a time leading to calibration errors. Fortunately, this discrepancy was measurable and a simple mathematical adjustment was implemented to remove the error.

The above stated power loss adjustment and detector calibration adjustment was written to a spreadsheet program to create a data recording template which was used to record, adjust, and normalize the reference power, transmitted power, and fluorescence signal.

The procedure for collecting transmission and fluorescence data was as follows. Prior to sensing experiments, the length of fiber was wiped clean with an acetone soaked Kimwipe. Transmission and fluorescence data was first collected with a length of the fiber submerged in pure ethylene glycol which has an index of refraction of 1.43 leading to a critical angle, θ_c, of approximately 54 degrees according to Equation 1.1. Detector R was dropped into position behind the chopper and the laser power was set to a predetermined value. This value was recorded by the laptop four times with six seconds

between each measurement to allow time for the oscilloscope to average. Detector R was lifted from the beam path and the transmission and fluorescence signal were recorded simultaneously by the laptop again measuring four times with six seconds between each measurement. To ensure the stability of the laser over the four measurements, Detector R was dropped back into the beam path and the reference was recorded by the laptop. If the reference drifted, the experiment was repeated. The spreadsheet program automatically averaged and normalized the eight values for the reference and the four values for the transmission as well as the four values for the fluorescence. The fiber was then removed from the ethylene glycol and the sensing region was rinsed in pure acetone. The above procedure was then repeated with a fluorescent dye solution. The dye solution was made by adding methanol drop-wise to rhodamine perchlorate 610 crystals until the crystals were fully dissolved. The dye-saturated methanol was then diluted with pure ethylene glycol to make a one milli-molar mixture of rhodamine perchlorate dye solution. After data was collected with a length of the fiber submerged in the fluorescent dye, the fiber was removed and rinsed in pure acetone then soaked in pure acetone until the fluorescence signal returned to baseline and a stain was no longer visible on the fiber. Soak time ranged from minutes to an hour for different fibers.

3.2 Effect of Coiling on Sensitivity

The same apparatus and procedure were used to collect data to determine the effect of coiling the fiber. However, for these experiments the fiber was carefully coiled around a trimmed nylon rod.

A 7/8 inch diameter, threaded 6/6 nylon rod with 9 teeth per inch was cut as shown in Figure 3.2 and secured to a metal rod. A wire was wrapped around the threaded piece to create holes to guide and secure the fiber coils. The diameter of the coils was chosen in the preliminary stage of this research to prevent breaking the fiber. Latex finger cots were used to handle the fiber while coiling so as to prevent contaminating the surface of the fiber. Care was taken to position the coils so that the sensing region was the same region and length used in those experiments where the fiber was straight. To submerge the coils in fluid, a beaker was raised from below the coils with a laboratory jack. Data was collected using the same procedure as in the previous experiment.

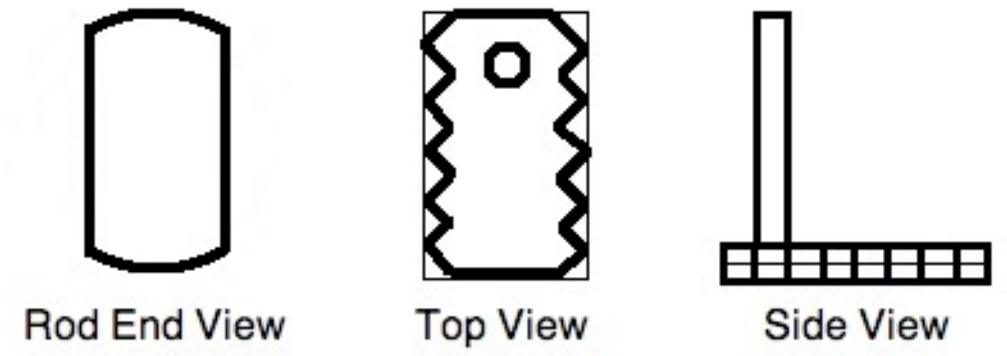

Figure 3.2 Threaded Nylon Rod Mounted to Metal Rod

3.3 Fiber Diameter Measurement

The diameter of the fibers was measured using a JEL JSM-6390LV scanning electron microscope. The fibers were first wiped with an acetone soaked Kimwipe then 1.5 centimeter lengths were broken from each fiber and mounted to an aluminum SEM target using copper tape. The samples were sputtered with a ten angstrom layer of gold palladium to prevent surface charging. The diameter of the fiber was measured every 100 microns using the microscope's software.

CHAPTER 4

DISCUSSION OF RESULTS

4.1 Effect of Diameter Fluctuations on Sensitivity

Data were collected for two groups of fibers. Fibers 1, 2, and 3 were approximately 60 microns in diameter while Fibers 4, 5, and 6 were approximately 75 microns in diameter. Diameter fluctuations measured using the SEM can be seen in Figures 4.1 and 4.2. Due to limitations of the SEM sample size, only about 7mm of fiber could be examined and it was assumed that the SEM sample was a good representation of the fiber's entire length. Visible observations supported this assumption since diameter fluctuations could be seen with the naked eye as shown in Figure 4.3. In this photograph, modulations in the amplitude of the light scattering from the surface of a fiber can be seen with a period of approximately six millimeters. Despite appearing thicker in the photograph, the brighter sections are actually down-tapers converting lower order modes to higher order modes that leak out of the fiber. This is further observed in Figure 4.4 which is a strongly fluctuated fiber submerged in fluorescent dye solution. The source is propagating from right to left and small cones of light can be seen escaping the brighter sections of the fiber. Furthermore, the data on Table 4.1 shows that fibers with stronger diameter fluctuations experience greater transmission loss due to the tapers converting lower order modes to higher order modes. The transmission loss is the percent change of transmission from pure ethylene glycol to fluorescent dye solution.

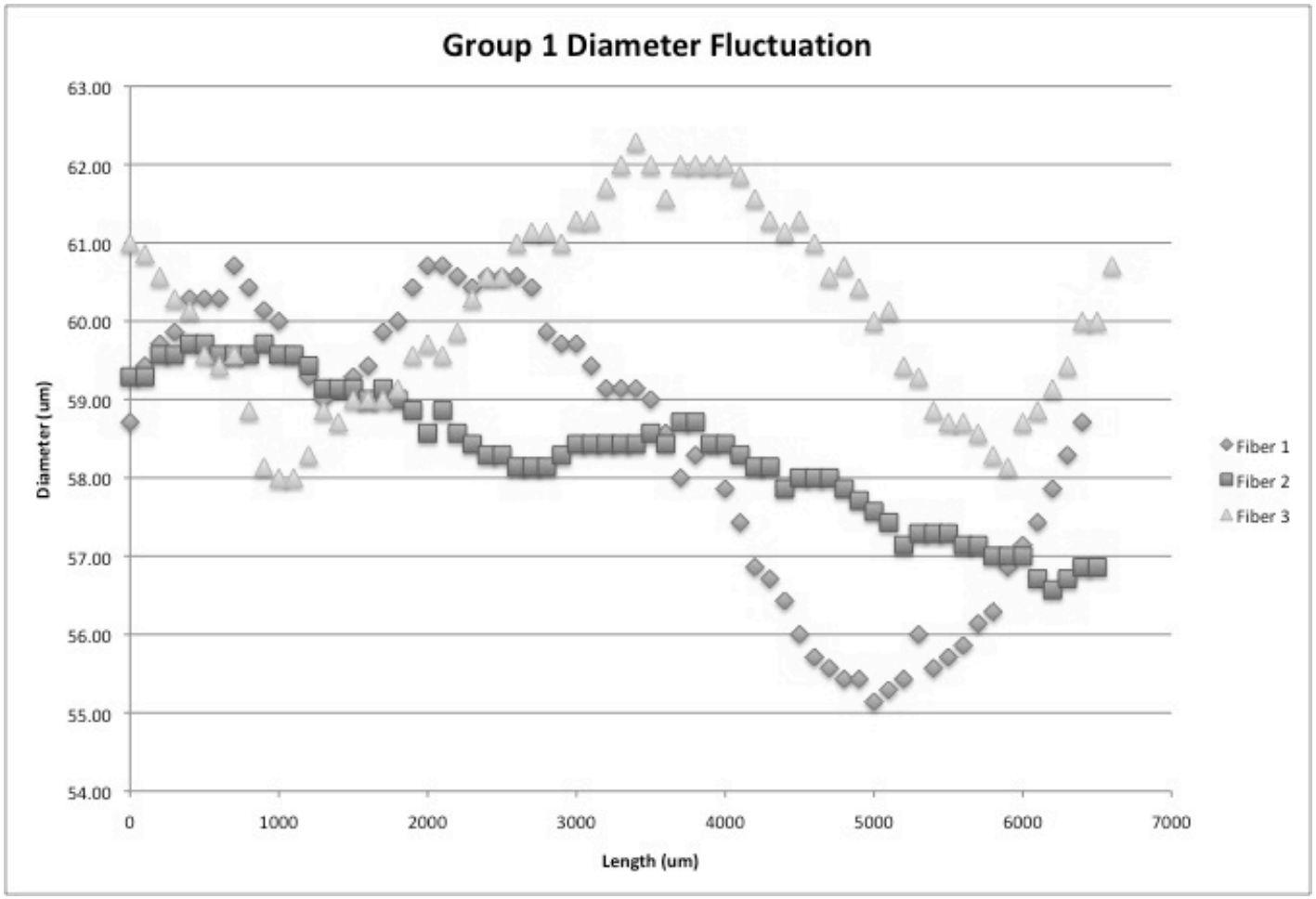

Figure 4.1 – Group 1 Diameter Fluctuation

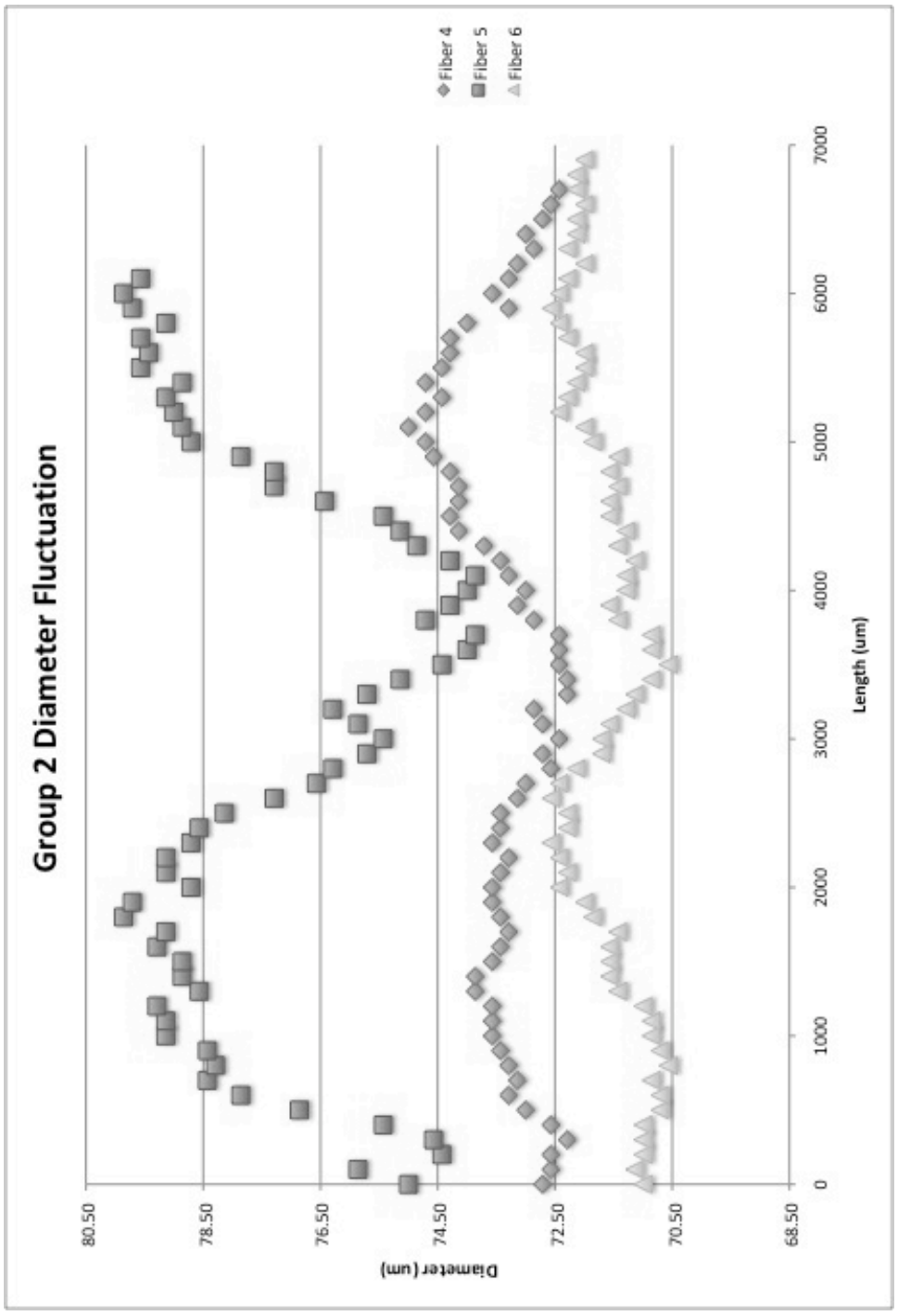

Figure 4.2 – Group 2 Diameter Fluctuation

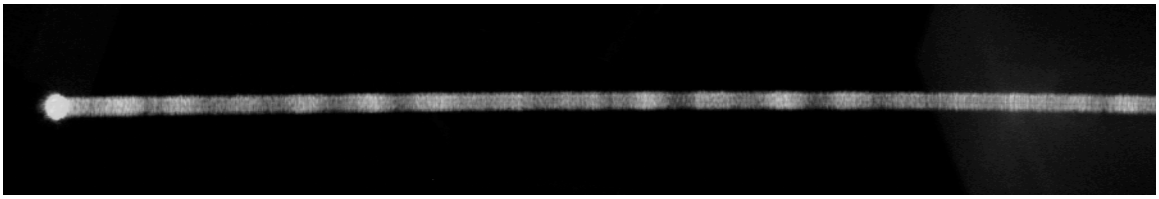

Figure 4.3 – Intensity Modulation Due to Diameter Fluctuations

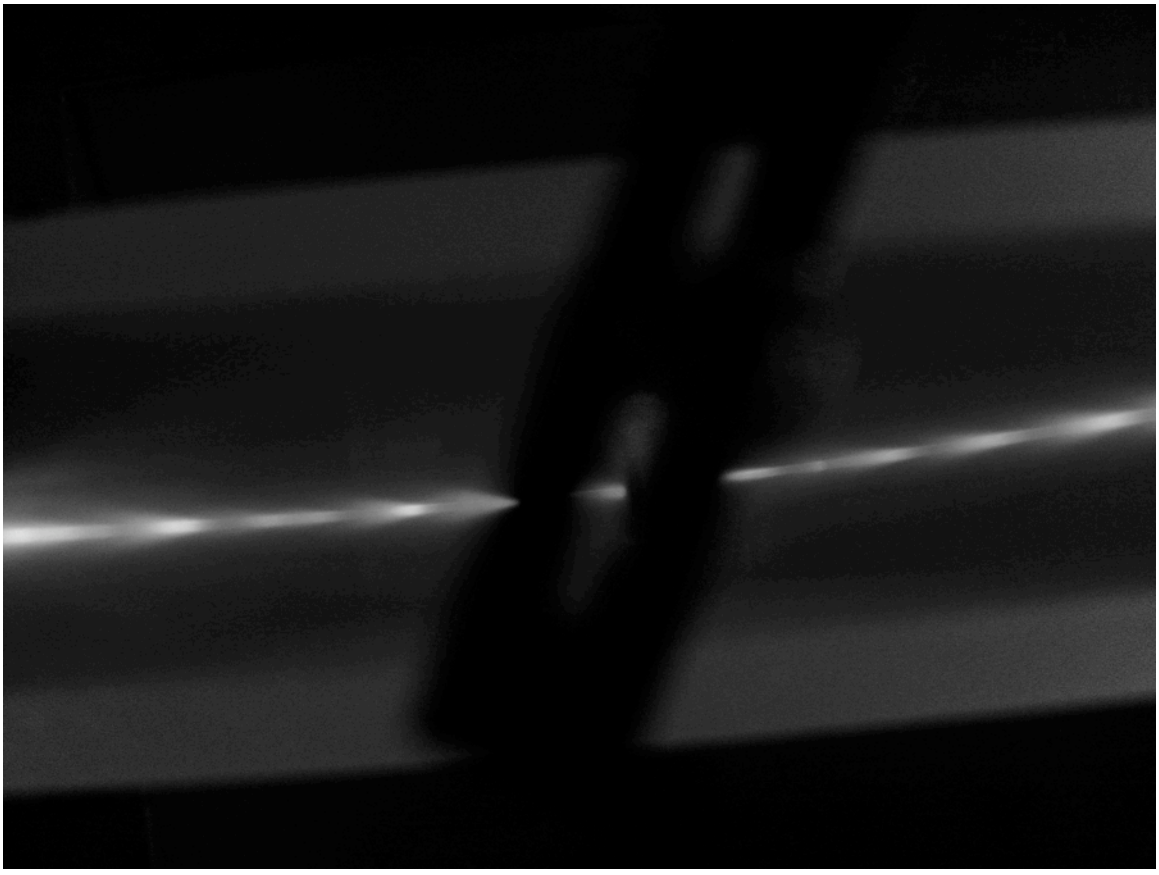

Figure 4.4 – Light Cones Escaping Down-tapers

	Fiber	Approximate Diameter (um)	Input Taper	Length of Sensing Region (cm)	Fluorescence Signal (mV)	Transmission Loss
	2	58.0	NO	7.5	1.73	3.93%
	1	58.0	NO	7.6	62.9	11.6%
Group 1	3	60.0	YES 125um	7.6	196	31.9%

	Fiber	Approximate Diameter (um)	Input Taper	Length of Sensing Region (cm)	Fluorescing Signal (mV)	Transmission Loss
	6	71.5	NO	12.5	6.72	9.60%
	4	73.5	NO	14.0	17.1	16.9%
Group 2	5	76.5	NO	12.5	26.4	20.9%

Table 4.1 – Fiber Characteristics and Collected Data for Straight Sensor

Table 4.1 also shows each fiber's characteristics and collected fluorescence sensitivity. In Group 1 Fiber 2 had the weakest diameter fluctuation corresponding to the weakest fluorescence sensitivity and lowest transmission loss. Fiber 3 had the strongest fluorescence sensitivity and greatest transmission loss due to its shorter period of fluctuation as well as its tapered input. It can be shown using Snell's Law and Equation 2.2 that a ray travelling in air incident on the input face of Fiber 3 with an angle of 29 degrees with respect to the fiber axis will enter the fiber and propagate with angle θ of 55 degrees which is close to the critical angle of approximately 54 degrees in solution. In contrast, for the fibers without a tapered input, the angle of incidence on the input face would have to exceed 90 degrees, an unrealistic situation, to propagate with θ equal to 55 degrees. Therefore, the combination of diameter fluctuation and tapered input allowed Fiber 3 to have a sensitivity over three times greater than that of Fiber 1 and two orders of magnitude greater than Fiber 2.

In the 75 micron group Fiber 5 had the strongest fluctuation, largest transmission loss, and largest fluorescence signal. Fiber 5's sensitivity is approximately four times greater than Fiber 6, which had the weakest fluctuation, lowest transmission loss, and weakest fluorescence signal. The transmission loss and fluorescence signal for Fiber 4 is between the values for Fibers 5 and 6 yet the diameter fluctuation for Fiber 4 is similar to that of Fiber 6. Further experimentation on Fiber 4 produced data in closer agreement to Fiber 6. This data is presented in Section 4.2.

It is evident that the sensitivities of Group 1 are greater than that of Group 2. This could be a consequence of Group 1 having a smaller diameter than Group 2. According

to Equation 1.2 a smaller diameter results in more bounces per unit length which increases the sensitivity of the sensor.

Based on this data, it can be assumed that the combination of diameter fluctuation, a tapered input, and a smaller diameter can significantly increase the sensitivity of the sensor. Of course, increasing the length of the sensing region will also increase the sensitivity. By experimentally adjusting these values, it may be possible to increase the sensitivity of the sensor by over two orders of magnitude.

For comparison, Table 4.2 shows the fluorescence signal and percent of transmission collected by immersing the output end of the most strongly fluctuated fibers into the fluorescent dye. The percent of transmission is the measured output power of the fiber divided by the input power. It can be seen that the input taper and shorter length of Fiber 3 significantly increases the output transmission and end fluorescence.

Further work in this area should focus on controlling the characteristics of the diameter fluctuations such that the evanescent fluorescence sensor sensitivity meets or exceeds the end fluorescence sensitivity.

Fiber	Approximate Diameter (um)	Input Taper	Length of Fiber (cm)	Percent Transmission	Fluorescence Signal (mV)
5	76.5	NO	28.5	16.9%	81.8
3	60	YES 125um	21.3	28.7%	489

Table 4.2 – End Fluorescence Data

4.2 Effect of Coiling on Sensitivity

It has also been shown that coiling the fiber can increase the sensitivity of sapphire fibers used in absorption sensing. However, this experiment did not show a significant increase in sensitivity. Instead, the experiment uncovered a number of unexpected phenomena complicating the experiment and leading to discoveries of previously unknown fiber characteristics.

Fiber 4 was the first fiber to be coiled and it was immediately apparent that the collected data was erratic (Table 4.3 – Trial 1). To eliminate the possibility of discrepancies due to changes in the launch angle, the fiber was not removed from the apparatus between experiments. Upon coiling the fiber, the transmission in ethylene glycol expectedly dropped as compared to the straight sensor. However, the transmission loss from pure ethylene glycol to the dye solution was unexpectedly low. The measured fluorescence signal was also low when compared to the fluorescence signal from the straight sensor. This data suggested that upon coiling the fiber an unknown mechanism prevented the evanescent wave from exciting the fluorescent molecules.

	Sensor	Transmission in Ethylene Glycol (mV)	Transmission in Dye Solution (mV)	Transmisison % Change from Ethylene Glycol to Dye	Fluorescence Signal (mV)
Trial 1	Pre-coil Length	639	531	-16.9%	17.1
	Coils	355	344	-3.14%	3.04
	Post-coil Length	440	446	1.54%	5.80
Trial 2	Pre-coil Length	560	484	-13.6%	8.58
	Coils	382	352	-7.69%	3.15
	Post-coil Length	442	459	3.86%	8.42
Trial 3 - Multiple EG Immersions	Pre-coil Length	575	501	-12.9%	8.83
	Coils	482	437	-9.37%	7.34
	Post-coil Length	557	493	-11.4%	8.68
Trial 4 - Multiple EG Immersions	Pre-coil Length	576	513	-10.9%	9.50
	Coils	453	414	-8.51%	6.00
	Post-coil Length	522	469	-10.2%	7.66
Trail 5	Pre-coil Length	566	495	-12.6%	8.85
	Coils	443	454	2.54%	10.5
	Post-coil Length	481	487	1.27%	10.3

Table 4.3 – Fiber 4 Transmission and Fluorescence Data

The fiber was uncoiled and data was collected using the straight length. The transmission in ethylene glycol increased but was still far below the initial pre-coil level. When immersed in the dye solution, the transmission actually increased above the level measured in pure ethylene glycol. There was no explanation for this behavior.

The fiber was left to sit for two days and the straight length was measured again (Table 4.3 – Trial 2). The measurement showed that the transmission of the fiber had increased without any external or experimenter influence. This suggested a time dependant anomaly.

To determine the cause of the transmission gain from pure ethylene glycol to the dye solution, an experiment was performed where the fiber was removed from the ethylene glycol, rinsed in acetone, and then placed back into the ethylene glycol (Table 4.3 – Trails 3 and 4). The transmission did indeed increase upon the second immersion in ethylene glycol. Also, the fluorescing signal for the coiled sensor in this experiment doubled.

Further experimentation showed that multiple immersions in ethylene glycol were necessary for both the coiled sensor and post-coil straight sensor transmission measurements. Without multiple immersions in ethylene glycol, the behavior would revert and the transmission in the dye solution would be higher than in the pure ethylene glycol (Table 4.3 – Trial 5). Interestingly, the fluorescence signal maintained its value. Furthermore, the post-coil straight sensor transmission was always lower than the pre-coil straight sensor transmission even after multiple immersions. However, the transmission always increased back to the same pre-coil level autonomously over a day's time. Also,

multiple immersions had no effect on the pre-coil straight sensor transmission; this phenomenon was only present in the coils and post-coil straight length.

The pre-coil straight sensor transmission levels of Trials 2 through 5 were lower than the initial transmission level of Trail 1 before the fiber had ever been coiled. This observation led to the idea that the stress of coiling may introduce microcracks into the surface of the fiber that could be responsible for some of the interesting data collected. Upon coiling the fiber for the first time, microcracks could develop which would increase scattering at the surface of the fiber and decrease the transmission. These microcracks could also fill with liquid upon coiling and uncoiling leading to the anomalous behavior of transmission increase with multiple immersions. Fluid filling these cracks would decrease the Fresnel reflection at the interfaces of the crack walls and the fluid thereby increasing the transmission. Dye solution filling these cracks would result in an increase in fluorescing signal, as some of the dye molecules would now be directly in the path of the internally guided light. Also, it was possible that the fiber relaxed overnight and the gaps of these microcracks would close up leading to the observed time dependant increase of transmission. To search for microcracks, it was necessary to inspect the surface of the fiber using a scanning electron microscope. The results of that inspection are explained in the Section 4.3.

Experiments were carried out on Fibers 5 and 6 with many of the same results. The extreme change in transmission and fluorescence signal upon initial coiling was not observed. However, the pattern of lower post-coil straight length transmission and "self-healing" over time were again evident. Also, it was again necessary to immerse the coiled fiber and post-coil length in ethylene glycol multiple times to increase and

stabilize the transmission. However, just as for Fiber 4, multiple ethylene glycol immersions had no effect on the pre-coil straight length. Table 4.4 shows the transmission loss and fluorescence signal of Fibers 5 and 6. For these fibers there were no significant changes in transmission loss and fluorescence signal versus the straight sensor.

Based on these observations it was concluded that coiling the fiber did not increase the sensitivity of the sensor. It is possible that fluorescence coupled into the coils is lost quickly while in the coils due to the conversion to higher order modes not conducive to propagation.

However, since coiling the fiber is essential to the design of a practical sensor, it was deemed necessary to further explore the possibility and consequence of microcracks on the surface of the fiber and attempt to explain the erratic behavior of Fiber 4 and the decrease of transmission due to repeated coiling.

	Fiber	Approximate Diameter (um)	Input Taper	Length of Sensing Region (cm)	Fluorescence Signal (mV)	Transmission Loss
	6	71.5	NO	12.5	6.66	11.1%
Group 2	5	76.5	NO	12.5	27.8	20.8%

Table 4.4 – Group 2 Coiled Fiber Characteristics and Collected Data

4.3 Scanning Electron Microscope Analysis of Fiber Surface

A scanning electron microscope was used to attempt to find microcracks on the surface of the fiber. However, instead of finding microcracks, the microscope revealed evidence of a surface layer of material coating the fiber. As shown in Figure 4.5 this layer has what appears to be a porous texture. Figure 4.6 shows the same region after being wiped with an acetone soaked Kimwipe. It appears that wiping the fiber has disturbed the surface layer leading to the belief that this layer is somewhat soft and can be removed with mechanical abrasion. However, a Kimwipe was too gentle to completely remove this layer. Figure 4.7 shows the fiber after being scraped with a piece of YAG. It is clearly evident that the surface layer has been severely disturbed with this more aggressive abrasion. Due to the fragility of the fiber, attempts were made to remove the surface layer by means of chemical attack.

A fiber sample was soaked in 25% hydrofluoric acid for one week and inspected. Figure 4.8 shows that the acid failed to completely remove the surface layer. In this image the surface was scraped with YAG to distinguish the remaining surface layer. The failure of the hydrofluoric acid to completely dissolve this layer suggests that the layer is composed of alumina.

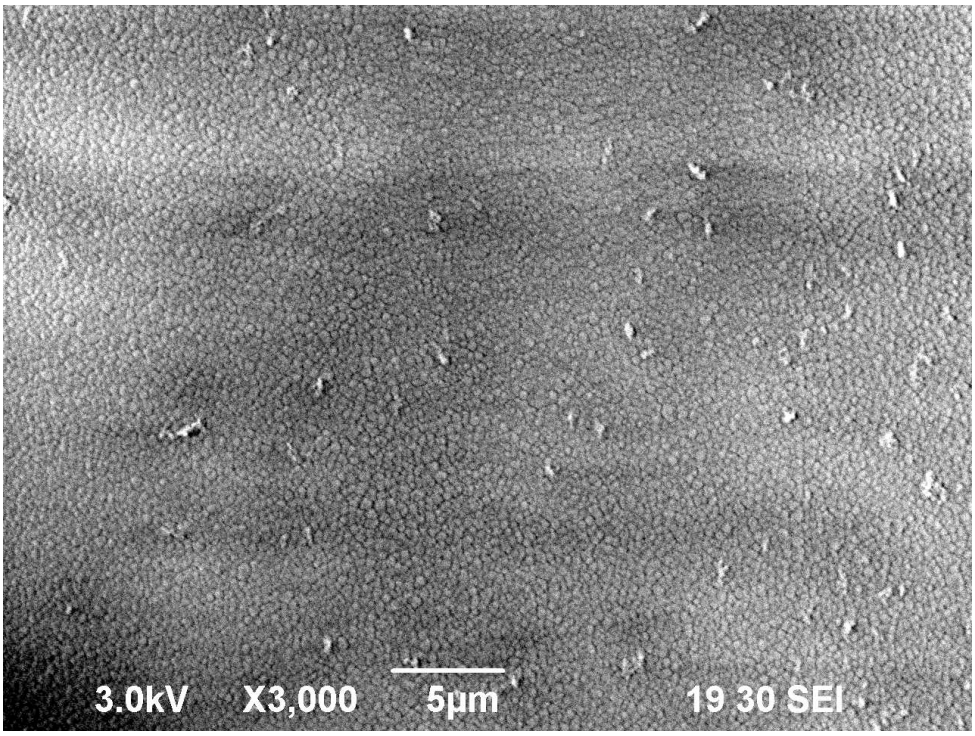

Figure 4.5 – Undisturbed Surface of Fiber

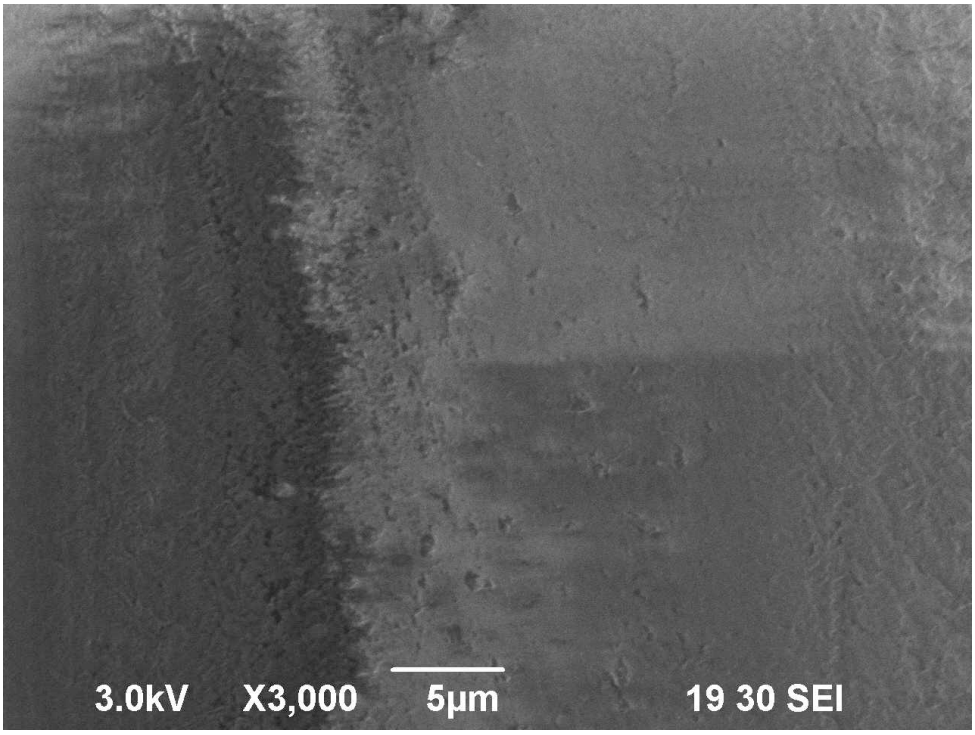

Figure 4.6 – Surface After Wiped with Acetone Soaked Kimwipe

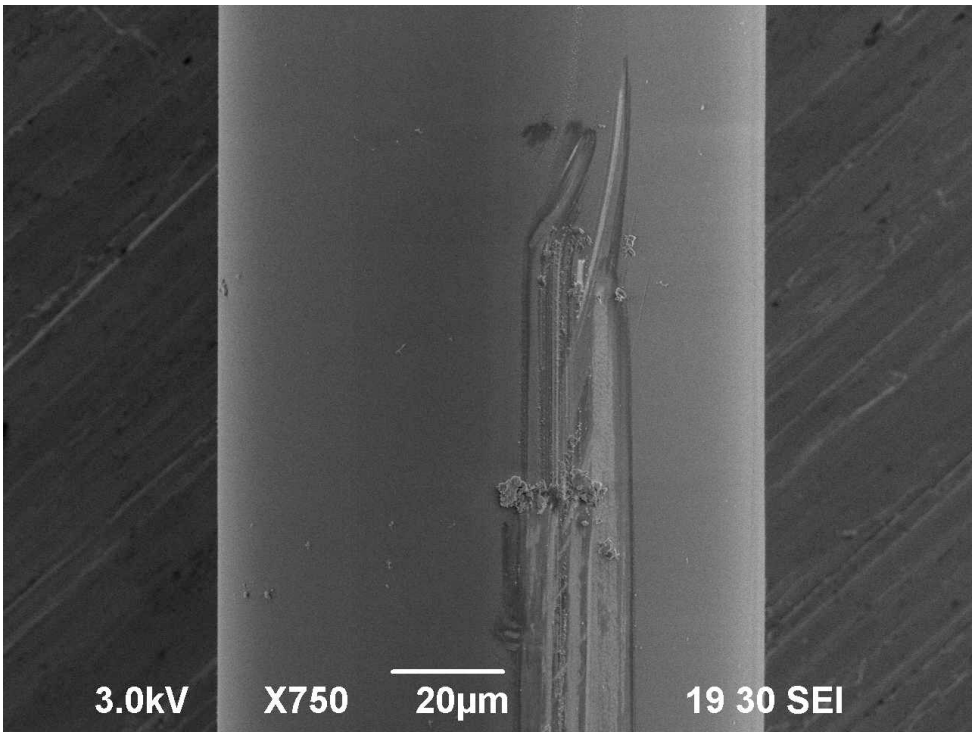

Figure 4.7 – Surface Scraped with YAG

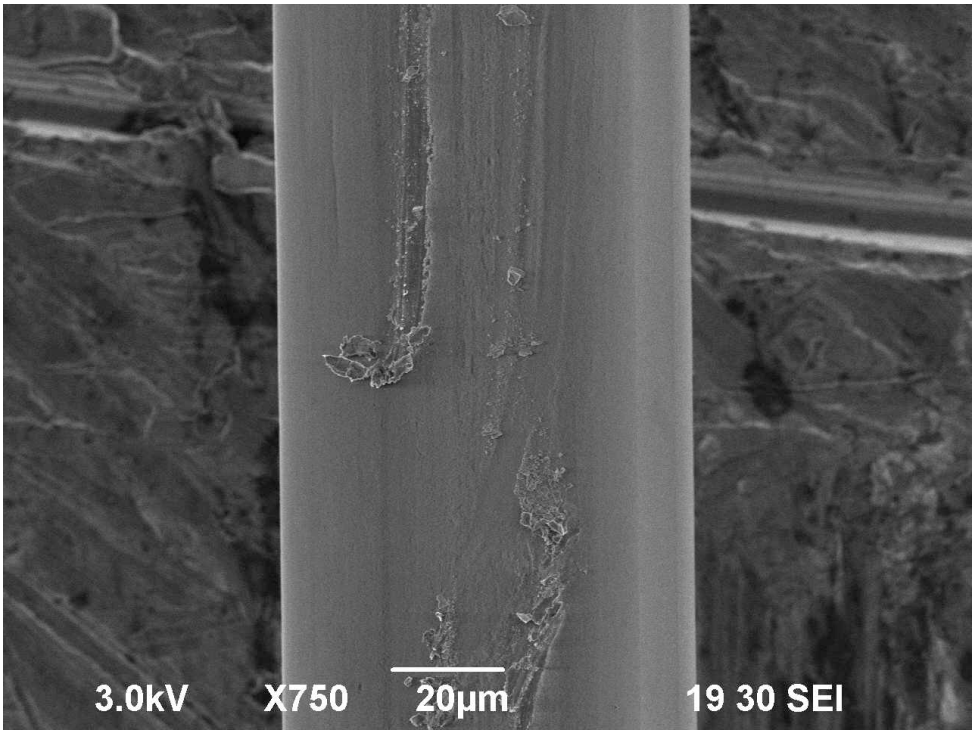

Figure 4.8 – YAG Scrape Shows Layer After One Week in 25% HF

Unfortunately, a method to completely remove the surface layer was not devised. However, it is assumed that this procedure would require mechanical abrasion using compounds such as silica that would abrade the surface layer without damaging the single crystal fiber beneath. It is possible that a hydrofluoric acid bath would further clean the surface by dissolving remnants of the surface layer without damaging the underlying single crystal structure.

As far as the composition and origin of this surface layer, without further investigation and experimentation, only preliminary ideas can be offered. MicroMaterials Inc. has reported that after growing a fiber, it is necessary to clean the inside of the growth chamber due to an accumulation of a fine layer of dust. Since the chamber is under vacuum during growth, the only source of this dust is from the vaporization of alumina from the molten zone. It is possible that this vaporized material escapes the molten zone and strongly bonds to the growing fiber immediately above the molten zone. Since the vaporized material is alumina, this would explain the layer's resistance to chemical attack.

In any case, the presence of this surface layer has a tremendous impact on the future of this research. If this layer is porous it may act as a sponge absorbing and trapping fluids. When the fiber is coiled, this layer may shift or crumple resulting in a surface terrain that consequently alters the evanescent field at the true surface of the fiber. The shifting of the surface layer could create voids and spaces that could fill with fluid. This may explain why multiple immersions in ethylene glycol only had an effect after coiling and again after uncoiling. Also, over time, these fluids could evaporate leading to the changes seen over a period of days. If the layer is indeed deposited from the

vaporization of material from the molten zone, this layer may be of differing thickness depending upon the temperature of the molten zone and the growth rate of the fiber.

It is possible that for the first few coilings of Fiber 4, this layer was extremely disrupted and effectively blocked the true surface of the fiber from the surrounding liquid. Perhaps after repeated handling, the layer was somewhat removed resulting in the sudden increase in fluorescence sensitivity while coiled.

Further study is necessary in this area to determine the exact consequences of this surface layer. The composition of this layer must be determined and this information will help isolate the origin of the layer. The layer must be removed and these experiments repeated to determine if the anomalous behavior was indeed caused by this layer. Also, the layer must be removed to inspect the fiber surface for microcracks. And ultimately, experiments must be performed to determine the effect of the surface layer on the fluorescence sensitivity of the sensor.

CHAPTER 5

CONCLUSION

Based on the results of the collected data, it is concluded that sapphire fibers grown with diameter fluctuations have a greater sensitivity than smooth fibers when used as evanescent wave fluorescence sensors. The increase in sensitivity is due to a series of bi-tapers that convert lower order modes into higher order modes thus increasing the evanescent penetration depth. These fibers efficiently couple the fluorescence back into the core and guide it to the ends of the fiber where it can be detected and measured.

Future work in this area should focus on controlling the diameter fluctuation during growth. It may be possible to modulate either the laser power or the speed of the growth motors to produce fibers with controlled diameter fluctuations. The depth of modulation as well as the period of fluctuation should be studied to maximize the sensitivity of the sensor.

It is also concluded that coiling the fiber did not increase the sensitivity of the sensor. This may be due to the loss of fluorescence within the coils due to mode conversion but may also be a consequence of a change in the surface terrain of the fiber's discovered surface layer.

Further research is required to determine the consequences of the surface layer on the sensor's sensitivity. This layer must also be removed and the true surface of the fiber must be inspected for surface microcracks that may develop under the stress of coiling.

REFERENCES

1. D. Bailey and E. Wright, Practical Fiber Optics, Newnes, 2003.

2. J. Tyndall, Notes on Light, Longmans, Green, and Company, 1870.

3. K. Kao and G. Hockham, Proceedings of the Institution of Electrical Engineers, 1151, 1966.

4. F. Yu and S. Yin, Fiber Optic Sensors, Marcel Dekker, Inc., 2002.

5. K. Iizuka, Elements of Photonics Vol. II, John Wiley and Sons, Inc., 2002.

6. E. Hecht, Optics, Addison Wesley, 2002.

7. A. Mignani, R. Falciai, and L. Ciaccheri, Applied Spectroscopy 52, 546, 1998.

8. R. Verma, A. Sharma, and B. D. Gupta, IEEE Photonics Technology Letters 19, 1786, 2007.

9. S. K. Khijwania and B. D. Gupta, Optical and Quantum Electronics 31, 625, 1999.

10. M. Grossman, Evanescent Field Absorption Sensing Using Sapphire Fibers, M.S. Thesis, 2007.

11. A. Snyder and J. Love, Optical Waveguide Theory, Chapman and Hall Ltd., 1983.

12. D. Woerdeman and R. Parnas, Applied Spectroscopy 55, 331, 2001.

13. R. Lieberman, L. Blyler, and L. Cohen, Journal of Lighwave Technology 8, 212, 1990.

14. P. Wiejata, P. Shankar, and R. Mutharasan, Sensors and Actuators B96, 315, 2003.

15. A. Fielding, and C. Davis, IEEE Photonics Technology Letters 14, 53, 2002.

16. C. Carniglia, L. Mandel, and K. Drexhage, Journal of the Optical Society of America 62, 479, 1972.

17. Y. Zaatar, et al., Materials Science and Engineering B74, 296, 2000.

18. A. Fielding, K. Edinger, and C. Davis, Journal of Lightwave Technology 17, 1649, 1999.

19. OSLO-EDU, Sinclair Optics, www.sinopt.com.

ABOUT THE AUTHOR

Jimmy Ray Gamez was born and raised in Rhinelander, Wisconsin. At age 19, he moved to Florida and enrolled in the Electronics Technology program at Withlacoochee Technical Institute in Inverness, Florida. He completed this 1400 program in approximately 950 hours with a 4.0 GPA and was recognized as the Outstanding Student in Electronics Technology. He then received his Associate's Degree in Secondary Education from Hillsborough Community College in Tampa, Florida and transferred to the University of South Florida where he received his Bachelor's Degree in Physics, Magna Cum Laude. With the completion of this thesis, Jimmy will receive his Master's Degree in Physics from the University of South Florida.